To cite this version :

Thierry PALIN-LUC, Serge LASSERRE - An energy based criterion for high cycle multiaxial fatigue - European Journal of Mechanics - A/Solids - Vol. 17, n°2, p.237-251 - 1998

An energy based criterion for high cycle multiaxial fatigue

Thierry PALIN-LUC and Serge LASSERRE*

ABSTRACT. – In spite of the great number of high cycle multiaxial fatigue criteria in the literature, none predicts the difference that exists between the endurance limits in traction, four point rotative bending and four point plane bending. An energy based criterion based on a new concept using the strain energy density is proposed in this paper. This new calculation method explains the previous differences by taking into account the volumic distribution of the strain energy density around the considered critical point in fatigue. This method, available now under fully reversed multiaxial loadings, also takes into account the stress state triaxiality. Under combined plane bending and torsion the predictions of the new proposal lead to Gough and Pollard's ellipse quadrant for ductile materials and lead to a curve close to an ellipse arc for brittle materials. Under other multiaxial loadings, predictions are always close to an ellipse quadrant dependent on the loading mode. This method has been tested on smooth cylindrical specimens with several materials; calculations are in very good agreement with multiaxial experimental data

1. Introduction

Many high cycle multiaxial fatigue criteria have been proposed in the literature and several studies have been devoted to a critical assessment of these criteria (Ballard *et al.*, 1995), (Bennebach, 1993) and (Papadopoulos, 1994), many references related to the criteria cited below can be found in these works. After a set of empirical formulae proposed by their authors to synthesize important fatigue test campaigns which were done at the end of the nineteenth century and in the first half of the twentieth century (Wöhler, Haigh, Locati, Gerber, Gough and Pollard, etc.) the existing criteria in high cycle fatigue can be devided in three categories. The criteria of the first one are based on the following physical observation: after initiation, a fatigue crack propagates first along a shear plane. According to Miller and Zachariah (1977) this is the propagation first step; the second one is the crack propagation in a plane perpendicular to the maximum tensile principal stress direction. Since the aim of many high cycle fatigue criteria is to predict crack initiation (not propagation), many authors assumed that fatigue crack initiation was governed by the shear stress. Referring to this idea the following criteria can be cited: Stulen-Cummings, Findley, Mc Diarmid, Sines, Crossland, etc. The criteria of the second set are based on the microscopic approach proposed for the first time by Dang Van in 1973. Since at a microscopic scale a metal is not isotropic nor homogeneous

but is constituted from crystals of random orientation, Dang Van considers that fatigue failure do not occurs if and only if the response of the grains most unfavorably oriented and subjected to the microscopic fluctuations of the loading is elastic shakedown. Based on this assumption the following criteria were proposed: Dang Van, Papadopoulos and Deperrois for instances. These calculation methods research a critical plane containing the easiest slip direction of the crystals. Finally, other authors considered that crack initiation can be described by an energetic quantity exceeding a critical value: Ellyin, Glinka for examples. The criteria of this last category are based on the total strain energy density or the plastic strain energy density dissipated in the material. The main advantage of all the criteria based on a critical plane is to predict the crack propagation direction after initiation. The energy based criteria can not predict such a direction because energy is a scalar but these criteria use a simple macroscopic approach which do not need a long computation time to determine the critical plane.

However, none of the existing calculation methods predicts the well-known experimental differences which can be observed in all metallic materials between the endurance limits in traction, four point rotative bending and four point plane bending. Massonnet (1955) demonstrated this phenomenon with a 0.35% carbon steel in plane bending and rotative bending; Barrault and Lasserre (1980) showed the same behaviour with a 35CD4 steel. This means that the relation between predictions and experiments is not bijective. The endurance limit is dependent on the stress distribution in the mechanical part. Furthermore, in order to be in correct agreement with experiments, any high cycle multiaxial fatigue criterion has to be phase independent in combined plane bending and torsion (Papadopoulos, 1994) as shown by the experimental data of Simbürger (1975) and Froustey and Lasserre (1989). According to the work of Simbürger, however, the endurance limit seems to be phase dependent in biaxial traction (combined traction and internal/external pressure on thin walled tube). The aim of this paper is to present a new concept and a new criterion capable of predicting these observations and distinguishing load modes. At the moment the proposal is available under any fully reversed loadings; the effect of mean stresses is being studied now; variable amplitude loadings will be considered next. But it has to be emphasized that a bijective relation between predictions and experiments is looking for with this calculation method. Having justified the chosen energetic approach, its goal is to predict crack initiation and not crack propagation direction, the basis of the new concept used to establish our proposal is presented. The proposed criterion is then developed, first for loadings involving uniaxial stress states and secondly for multiaxial conditions. A multiaxial stress state is defined with respect to the principal stress components. Finally, a comparison between test data and predictions is presented.

2. A new concept

By loading smooth specimens in blocks of plane bending and torsion alternatively applied until failure, at stress levels corresponding to the same life, Lasserre and Froustey (1992) found that fatigue life is the same as under plane bending loading alone or torsion alone. These authors show that several criteria based on the search of a specific critical

plane such as Sines, Crossland, Dang Van, Papadopoulos can not explain experiments with complex loading in blocks of different types (bending and torsion for instance). They proposed an energetic formula based on the accumulation of distorsion energy during a period of loading (Lasserre and Froustey, 1992). Bennebach's tests (1993) in blocks of bending and torsion on a spheroidal graphite cast iron also show the same thing.

In a recent paper Papadopoulos and Panoskaltsis (1994) proposed a stress gradient dependent high cycle multiaxial fatigue criterion which predicts differences between plane bending and traction but not between rotative bending and plane bending. This proposal and all the others do not distinguish between these different loading modes because they only consider the tensor of stresses at the critical point and do not take into account the volumic distribution of stresses around this point. In Figure 1 we can see that the distribution of stresses at any moment is the same in plane bending and in rotative bending. In rotative bending, however, all the points lying on a circle centred on the middle of the specimen cross-section support the same stress during a cycle. In plane bending there is no axisymmetry, there are only two points supporting the greatest
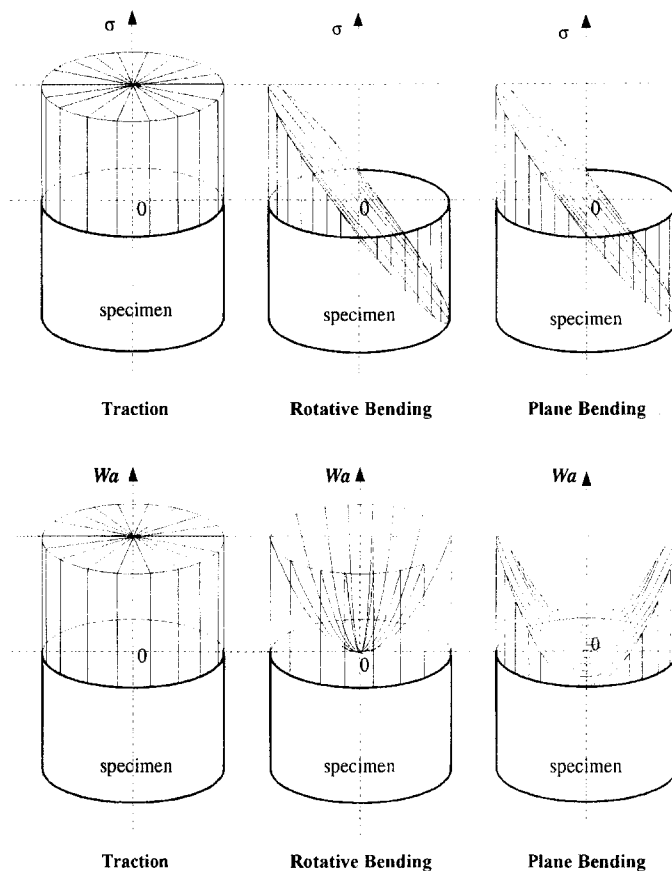

Fig. 1. – Stress distribution at a moment and *Wa* distribution on the cross-section
of a smooth specimen loaded in traction, rotative bending or plane bending.

stresses. Considering a complete loading cycle such as proposed by Tsybanev (1994) permits to take into account this observation.

In their fatigue criterion, Froustey *et al.* (1992) have considered a complete cycle of stresses; our proposal is based on their work. They use the mean value on one cycle of the volumic density of the elastic strain energy, *Wa*, defined by (1) whatever the point *M* in the mechanical part.

$$(1) \qquad Wa(M) = \frac{1}{T} \int_0^T \frac{1}{2} \sigma_{ij}(M, t) \, \varepsilon_{ij}^e(M, t) \, dt$$

where $\sigma_{ij}(M, t)$ and $\varepsilon_{ij}^e(M, t)$ are respectively the tensor of stresses and the tensor of elastic strains at the considered point M function of time. Usually the endurance limit is low enough to consider that the material remains elastic at the macroscopic scale (Lemaitre and Chaboche, 1988). Thus, *Wa* can be considered as the mean value on one cycle of the total strain energy density at the considered point. Figure 1 illustrates the Wa distributions on the cross-section of a smooth specimen loaded in traction, rotative bending and plane bending. These distributions are very different. In order to take into account these differences we propose to consider a volume element around the critical point; this volume is defined below.

Experimental observations and data help us to define this volume. Vivensang and Gannier (1994) carried on SEM observations on smooth specimens in 35CD4 annealed steel loaded in four point rotative bending. They observed that persistent slip bands already exist after 50,000 cycles and microcracks after 300,000 cycles at the surface of smooth specimens loaded at their endurance limit. This means that the material is damaged (in terms of microcrack) even if it is loaded at its endurance limit without any macroscopic crack. Cumulative damage tests in blocks (Palin-Luc, 1996) and (Palin-Luc *et al.*, 1997) on a spheroidal graphite cast iron prove that blocks with stress amplitude equal to the endurance limit participate to damage if they are mixed with higher blocks. But, if the stress amplitude of low blocks is lower than a specific value the fatigue life is the same as if the amplitude of the low blocks were equal to zero. Furthermore, a constant amplitude load below this specific value creates no observable microcrack in the matrix of the cast iron. These studies show that another limit, called σ^*, can be defined below the usual endurance limit of the material, σ^D. At a considered point a stress amplitude below this new limit does not initiate observable damage at the microscopic scale (no microcracks). Between σ^* and σ^D a stress amplitude only contributes to the initiation of micro damage, which could develop if, either near this point or in the course of time, there is a stress amplitude higher than the endurance limit. The usual endurance limit is a limit of no damage propagation but it is not a limit of no damage initiation.

From σ^* and by analogy with a sinusoidal traction load the corresponding mean value of the strain energy volumic density, Wa^*, can be calculated by (2), where E is the Young modulus of the material

$$(2) \qquad Wa^* = \frac{\sigma^{*2}}{4E}$$

According to the Froustey and Lasserre criterion, the critical points C_i with regard to fatigue are those where Wa is maximum. Around each point it is always possible to define the volume $V^*(C_i)$ by the set of points M where $Wa(M)$ is higher than $Wa^*(C_i)$ (see 3). We postulate that the part of $Wa(M)$ exceeding $Wa^*(C_i)$ is the damaging part of the strain energy volumic density. From $V^*(C_i)$, $\varpi_a(C_i)$ is defined by (4). $\varpi_a(C_i)$ is the volumic mean value of the strain energy volumic density around the critical point C_i.

(3) $V^*(C_i) = \{\text{points } M(x, y, z) \text{ around } C_i \text{ such that } Wa(M) \geq Wa^*(C_i)\}$

(4) $$\varpi_a(C_i) = \frac{1}{V^*(C_i)} \int \int \int_{V^*(C_i)} [Wa(x, y, z) - Wa^*(C_i)]\, d\nu$$

3. Uniaxial stress states

At the endurance limit and at the critical point C_i, this new quantity $\varpi_a(C_i)$ is supposed to be constant, whatever the uniaxial stress state. If we note $\varpi_a^D(Uniax)$ its value at the endurance limit for any uniaxial stress state our criterion can be written by inequation (5). Failure occurs if this inequation is not verified.

(5) $$\varpi_a(C_i) < \varpi_a^D(Uniax)$$

3.1. EXAMPLES ON SMOOTH CYLINDRICAL SPECIMENS

To apply this criterion, the following parameters have to be identified: σ^*, $Wa^*(Uniax)$ and $\varpi_a^D(Uniax)$. As there is no stress gradient along the longitudinal axis of a smooth cylindrical specimen, the volume V^* can be reduced to the surface S^* inside the specimen cross-section, Eqs. (3) and (4) become:

(6) $S^* = \{\text{points } M(x, y, z) \text{ around } C_i \text{ such that } Wa(M) \geq Wa^*(C_i)\}$

(7) $$\varpi_a(C_i) = \frac{1}{S^*(C_i)} \int \int_{S^*(C_i)} [Wa(x, y, z) - Wa^*(C_i)]\, ds$$

The Wa distributions are axisymmetric in traction and in rotative bending (Fig. 1) and for this reason these two sinusoidal loadings are taken in reference to identify σ^*. In traction, all the points of the cross-section of the specimen have the same Wa value (Fig. 2), expression (7) becomes:

(8) $Wa(Trac) = \dfrac{\sigma_{Trac}^2}{4E} \Rightarrow \varpi_a(Trac) = Wa(Trac) - Wa^*(Uniax) = \dfrac{\sigma_{Trac}^2 - \sigma^{*2}}{4E}$

In four point rotative bending S^* is a crown, the iso-Wa lines are circles as shown in Figure 2. For such a loading on smooth cylindrical specimens ϖ_a is given by (9) where

$\sigma_{RotBend}$ is the maximum stress due to rotative bending on the cross-section and ρ^* is the radius of the circle representing the iso-Wa* line (Fig. 2).

$$(9) \qquad Wa\,(RotBend) = \frac{\sigma^2_{RotBend} \cdot r^2}{4\,E \cdot R^2}$$

$$\Rightarrow \varpi_a\,(C_i,\,RotBend) = \frac{\sigma^2_{RotBend}}{8\,E} \cdot \left(1 - \left(\frac{\rho^*}{R}\right)^2\right) \quad \text{if } \rho^* < R$$

At the endurance limit, $\varpi_a\,(C_i)$ is supposed to be constant whatever the uniaxial stress state at the critical point C_i : $\varpi_a^D\,(Trac) = \varpi_a^D\,(C_i,\,RotBend)$. Thus equation (10) is obtained from (8) and (9); it is a convenient expression for design purposes. From (2) and (8) it is easy to prove that $Wa^*\,(Uniax)$ is given by (11); $\varpi_a^D\,(Uniax)$ can be calculated by (12).

$$(10) \qquad \sigma^* = \sqrt{2\,(\sigma^D_{Trac})^2 - (\sigma^D_{RotBend})^2}$$

$$(11) \qquad Wa^*\,(Uniax) = \frac{2\,(\sigma^D_{Trac})^2 - (\sigma^D_{RotBend})^2}{4\,E}$$

$$(12) \qquad \varpi_a^D\,(Uniax) = \frac{(\sigma^D_{RotBend})^2 - (\sigma^D_{Trac})^2}{4\,E}$$

Equation (10) is only available if $\sigma^D_{RotBend}/\sigma^D_{Trac} < \sqrt{2}$; according to the authors this condition is true on all metallic materials, usually this ratio is less than 1.3 (Papadopoulos and Panoskaltsis, 1994). $\sigma^D_{RotBend}$ can be considered as a material parameter if the radius of the specimen is larger than about 5 mm as shown by Pogorotskii and Karpenko (from Papadopoulos and Panoskaltsis, 1994).

Traction   Rotative Bending   Plane Bending

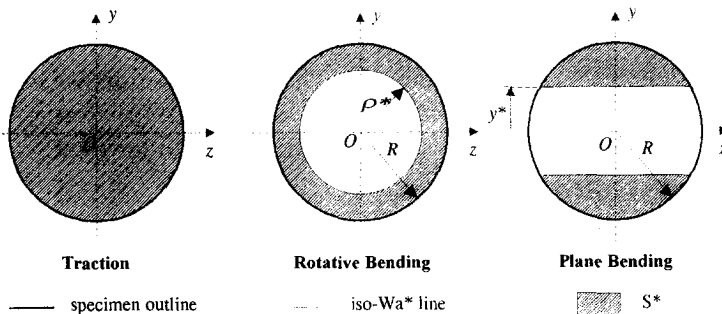—— specimen outline   ···· iso-Wa* line   ▨ S*

Fig. 2. – Iso-Wa lines and S^* surfaces on the cross-section
of a specimen loaded in traction, four point rotative bending or plane bending.

The iso-Wa lines are straight lines parallel to the neutral fibre of the cross-section (Fig. 2). Expression (13) can be deduced from (6) and (7), where σ_{PlBend} is the maximum stress on the cross-section due to plane bending and y^* is the ordinate of the iso-Wa* line (Fig. 2).

(13)

$$W a\,(PlBend) = \frac{\sigma_{PlBend}^2 \cdot y^2}{4\,E \cdot R^2} \quad \Rightarrow \quad \varpi_a\,(C_i,\,PlBend) = \frac{\sigma_{PlBend}^2}{4\,E} \cdot \{A\,(\alpha) - \alpha^2\}$$

$$\text{where} \quad \alpha = \frac{y^*}{R} \quad \text{and} \quad A\,(\alpha) = \frac{\dfrac{\pi}{8} - \dfrac{\alpha}{4}\,(2\,\alpha^2 - 1)\,\sqrt{1 - \alpha^2} - \dfrac{1}{4}\,\arcsin \alpha}{\dfrac{\pi}{2} - \alpha\,\sqrt{1 - \alpha^2} - \arcsin \alpha}$$

According to the previous hypothesis, $\varpi_a^D\,(Uniax) = \varpi_a^D\,(C_i,\,PlBend)$. By noting $\gamma = \sigma_{PlBend}^D/\sigma_{RotBend}^D$ the ratio we are looking for, this ratio is solution of Eq. (14) where $A\,(x)$ is the function defined by (13).

(14)

$$\varpi_a^D\,(Uniax) = \varpi_a^D\,(C_i,\,PlBend) \quad \Leftrightarrow \quad 2\,\gamma^2 \cdot A\left(\frac{\rho^*/R}{\gamma}\right) - \left(\frac{\rho^*}{\gamma}\right)^2 - 1 = 0$$

$$\text{where} \quad \frac{\rho^*}{R} = \sqrt{\frac{2\,(\sigma_{Trac}^D)^2 - (\sigma_{RotBend}^D)^2}{(\sigma_{RotBend}^D)^2}}$$

4. Multiaxial stress states

The influence of the triaxiality of stresses on the endurance limit has already been shown in a number of studies: Galtier and Séguret (1990) for instance. We propose to take into account this influence by using the F function defined by Froustey et al. (1992). By referring to the work of De Leiris (1969) these authors define the degree of triaxiality, dTa, for a fully reversed loading by expression (15) where Wsa and Wda are respectively the spherical part and the deviatoric part of the strain energy volumic density (16). For any periodic loading it is easy to prove that $Wa = Wsa + Wda$.

(15)
$$dTa = \frac{Wsa}{Wsa + Wda}$$

(16)

$$Wsa = \left(\frac{1 - 2\,v}{6\,E}\right) \frac{1}{T} \int_0^T I_{1a}^2\,(t)\,dt \quad \text{and} \quad Wda = \left(\frac{1 + v}{E}\right) \frac{1}{T} \int_0^T J_{2\,a}\,(t)\,dt$$

where $I_{1a}\,(t) = \sigma_{kk}\,(t)$ and $J_{2\,a}\,(t) = \frac{1}{2}\,s_{ij}\,(t)\,s_{ij}\,(t)$ by noting

$$\sigma_{ij}\,(t) = \frac{\sigma_{kk}\,(t)}{3} \cdot \delta_{ij} + s_{ij}\,(t).$$

Based on many experimental data in high cycle fatigue, Froustey et al. (1992) have proposed to relate, at the endurance limit, the value of $Wa\,(C_i,\,load)$, whatever

the loading, to the value of Wa in Torsion, $Wa\,(C_i,\,Tors)$, by the function F (see 17) depending on the degree of triaxiality of the stresses at the critical point C_i, $dTa\,(C_i,\,load)$, and a new material dependent parameter β.

$$(17) \quad F\,(dTa\,(C_i,\,load),\,\beta) = \frac{Wa^D\,(C_i,\,load)}{Wa^D\,(C_i,\,Tors)}$$

$$= \frac{1}{1 - dTa\,(C_i,\,load)} \cdot \left\{ 1 - \frac{1}{\beta} \cdot \ln\left[1 + dTa\,(C_i,\,load) \cdot (e^\beta - 1) \right] \right\}$$

The β parameter is representative of the material triaxiality sensitivity. β is equal to zero for a XC18 annealed steel and is around 3 for a spheroidal graphite cast iron. Evolution of the function F is illustrated by Figure 3. The identification of the β parameter has to be done by applying Eq. (17) with the endurance limits in Rotative Bending and in Torsion. It becomes (18) where the only unknown is β; v is the Poisson ratio. The endurance limit in torsion is the only other experimental data needed to apply this approach.

$$(18) \quad \frac{Wa^D\,(C_i,\,RotBend)}{Wa^D\,(C_i,\,Tors)} = \frac{1}{1 - \dfrac{1 - 2\,v}{3}} \cdot \left\{ 1 - \frac{1}{\beta} \cdot \ln\left[1 + \frac{1 - 2\,v}{3} \cdot (e^\beta - 1) \right] \right\}$$
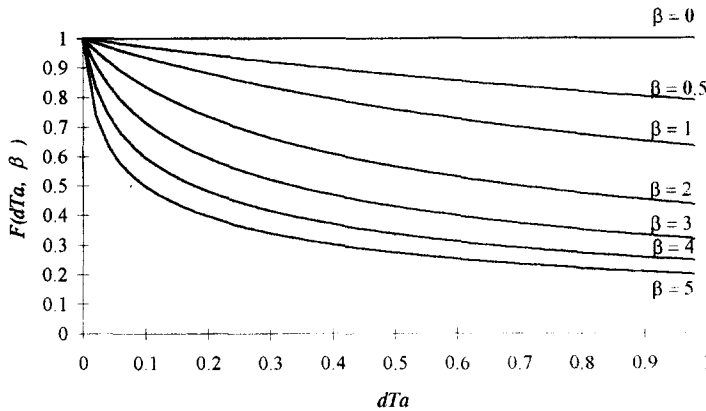

Fig. 3. – Evolution of the function F.

In order to take into account the triaxiality influence we suppose that Wa^* is loading dependent and verifies Eq. (19). It can be noted that in traction, rotative bending and plane bending, $dTa\,(C_i,\,load)$ is the same and so Wa^* has the same value. With (19) Wa^* is defined whatever the loading, so V^* is also defined.

$$(19) \qquad \frac{Wa^*\,(C_i,\,load)}{Wa^*\,(C_i,\,Tors)} = F\,(dTa\,(C_i,\,load),\,\beta)$$

The influence of triaxiality has also to be taken into account in the definition of the limit value of $\varpi_a^D(C_i)$. By analogy with the previous assumption, we postulate that for any loading at the endurance limit the value of $\varpi_a^D(C_i)$, noted $\varpi_a^D(C_i,\,load)$, verifies (20).

(20)
$$\frac{\varpi_a^D(C_i,\,load)}{\varpi_a^D(C_i,\,Tors)} = F(dTa(C_i,\,load),\,\beta) \;\Rightarrow\; \frac{\varpi_a^D(C_i,\,load)}{\varpi_a^D(Uniax)} = \frac{F(dTa(C_i,\,load),\,\beta)}{F(dTa(Uniax),\,\beta)}$$

With this last point the criterion can be applied on any fully reversed loading. Its use can be summarized as described below.

Use of this proposal

Two static characteristics of the material are necessary: E and v. Only three experimental endurance limits under fully reversed loadings are needed: the endurance limit in traction, σ_{Trac}^D, the endurance limit in rotative bending, $\sigma_{RotBend}^D$ and the endurance limit in torsion, $\tau_{T_0}^D$. From $\sigma_{RotBend}^D$ and $\tau_{T_0}^D$, the β material parameter is identified by solving Eq. (18). At the endurance limit on any mechanical part, the terms of the stress tensor are solutions of Eq. (20). In this equation $\varpi_a^D(C_i,\,load)$ is defined by:

(21)
$$\varpi_a^D(C_i,\,load) = \frac{1}{V^*(C_i)} \int\int\int_{V^*(C_i)} [Wa(x,\,y,\,z,\,load) - Wa^*(C_i,\,load)]\,dv$$

where $\quad V^*(C_i) = \{\text{points } M(x,\,y,\,z) \text{ such that } Wa(M) \geq Wa^*(C_i,\,load)\}$

and $\;Wa^*(C_i,\,load) = Wa^*(Uniax)\dfrac{F(dTa(C_i,\,load),\,\beta)}{F(dTa(Uniax),\,\beta)}$

The use of this criterion in a design department can be synthesized as shown in Figure 4.

5. Application of the criterion under combined loadings

The predictions of our proposal are presented below for several combined loadings usually used in laboratory tests. Calculations are detailed in combined rotative bending and torsion. For the other combined loadings: plane bending and torsion, traction and torsion, biaxial traction on thin walled tubes (traction and internal/external pressure) final results only are presented.

5.1. COMBINED ROTATIVE BENDING AND TORSION ON SMOOTH CYLINDRICAL SPECIMEN

On a smooth cylindrical specimen loaded at its endurance limit $(\sigma_{RotBend+T_0}^D,$ $\tau_{RotBend+T_0}^D)$ with $\sigma_{RotBend+T_0}^D/\tau_{RotBend+T_0}^D = k$ the Wa distribution on the specimen cross-section is given by expression (22).

(22) $\quad W_a(RotBend + T_0) = \left(\dfrac{r}{R}\right)^2 \cdot \left[\dfrac{(\sigma_{RotBend+T_0}^D)^2}{4\,E} + \left(\dfrac{1+v}{2\,E}\right)(\tau_{RotBend+T_0}^D)^2\right]$
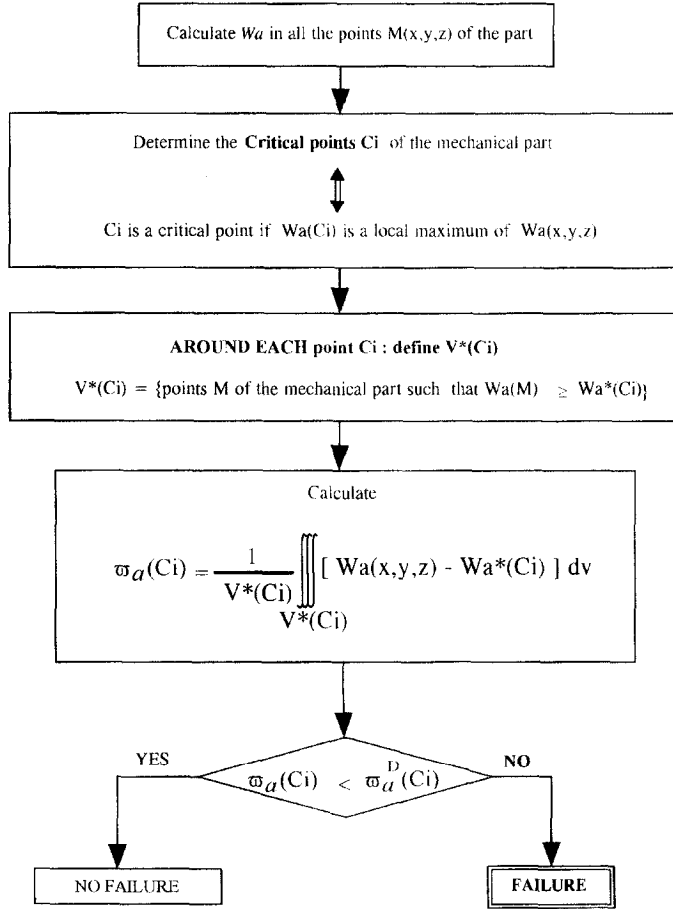
Fig. 4. – Synoptic of our proposal for use in a design department.

The $Wa^* (C_i)$ value in combined Rotative Bending and Torsion is given by:

(23)

$$W_a^* (C_i, RotBend+To) = \frac{2 (\sigma_{Trac}^D)^2 - (\sigma_{RotBend}^D)^2}{4 E} \cdot \frac{F (dTa (C_i, RotBend + To), \beta)}{F (dTa (Uniax), \beta)}$$

So by using (22) and (23) it is easy to prove that the r^* radius of the circle on the cross-section representing the iso-Wa* line is given by:

(24)

$$\left(\frac{r^*}{R} \right)^2 = \frac{2 (\sigma_{Trac}^D)^2 - (\sigma_{RotBend}^D)^2}{(\sigma_{RotBend+To}^D)^2 \cdot (1 + 2 \cdot (1 + v)/k^2)} \cdot \frac{F (dTa (C_i, RotBend + To), \beta)}{F (dTa (Uniax), \beta)}$$

From its definition (21) $\varpi_a^D\,(C_i,\ RotBend + To)$ is given by the following expression (25):

$$(25)\quad \varpi_a^D\,(C_i,\ RotBend + To) = \frac{(\sigma_{RotBend+To}^D)^2}{8\,E}\left(1 + \frac{2\,(1+v)}{k^2}\right)$$

$$+\frac{2\,(\sigma_{Trac}^D)^2 - (\sigma_{RotBend}^D)^2}{8\,E}\cdot\frac{F\,(dTa\,(C_i,\ RotBend+To),\beta)}{F\,(dTa\,(Uniax),\ \beta)} - Wa^*\,(C_i,\ RotBend+To)$$

and its value is defined by expression (26).

(26)
$$\varpi_a^D\,(C_i,\ RotBend+To) = \frac{(\sigma_{RotBend}^D)^2 - (\sigma_{Trac}^D)^2}{4\,E}\cdot\frac{F\,(dTa\,(C_i,\ RotBend+To),\ \beta)}{F\,(dTa\,(Uniax),\ \beta)}$$

From (25) and (26) and by using (23) the endurance limits $(\sigma_{RotBend+To}^D,\ \tau_{RotBend+To}^D)$ can be calculated. They are given by (27) whatever the ratio k.

$$(27)\quad \begin{cases} \sigma_{RotBend+To}^D = \sqrt{\dfrac{(\sigma_{RotBend}^D)^2}{1 + 2\,(1+v)/k^2}\cdot\dfrac{F\,(dTa\,(C_i,\ RotBend+To),\ \beta)}{F\,(dTa\,(Uniax),\ \beta)}} \\[2ex] \tau_{RotBend+To}^D = \dfrac{\sigma_{RotBend+To}^D}{k} \end{cases}$$

These predictions are phase independent because the degree of triaxiality is not phase dependent.

$$(28)\qquad dTa\,(C_i,\ RotBend + To) = \frac{(1 - 2\,v)\cdot k^2}{3\cdot k^2 + 6\cdot(1+v)}$$

Furthermore, these predictions lie on a curve all the closer to the Gough *et al.* (1951) ellipse quadrant, $(\sigma_{RotBend+To}^D/\sigma_{RotBend}^D)^2 + (\tau_{RotBend+To}^D/\tau_{To}^D)^2 = 1$, than the β parameter is close to zero (ductile material). β is all the more different from zero than the material is brittle; in this case the predictions are close to the Gough *et al.* (1951) ellipse arc.

5.2. OTHER COMBINED LOADINGS

5.2.1. *Plane bending and torsion, traction and torsion*

The results derived from our approach are dependent on the mode of loading; its predictions are different for each of these combined loadings, as illustrated by Figure 5. This method leads to three curves close to ellipse quadrants which are not phase dependent. This is in agreement with experiments.

5.2.2. *Biaxial traction on thin walled tube (traction and internal/external pressure)*

The longitudinal stress is $\sigma_l \sin \omega t$ and the hoop stress is $\sigma_h \sin(\omega t + \varphi)$ with $\sigma_l/\sigma_h = \lambda$. It must be pointed out that in biaxial traction on a thin walled tube the degree of triaxiality defined by (15) is phase dependent (*see* 29). Under this loading the endurance limits predicted by the criterion are phase dependent (30). They lie on a curve close to an ellipse arc as shown in Figure 5.

$$(29) \qquad dTa\left(C_i, BiaxTrac\right) = \left(\frac{1 - 2v}{3}\right) \cdot \left(\frac{\lambda^2 + 2 \cdot \lambda \cdot \cos\varphi + 1}{\lambda^2 - 2 \cdot v \cdot \lambda \cdot \cos\varphi + 1}\right)$$

$$(30) \quad \sigma_l^D = \sigma_{Trac}^D \sqrt{\frac{1}{1 + 1/\lambda^2 - 2\left(v\cos\varphi\right)/\lambda} \cdot \frac{F\left(dTa\left(C_i, BiaxTrac\right), \beta\right)}{F\left(dTa\left(Uniax\right), \beta\right)}}$$

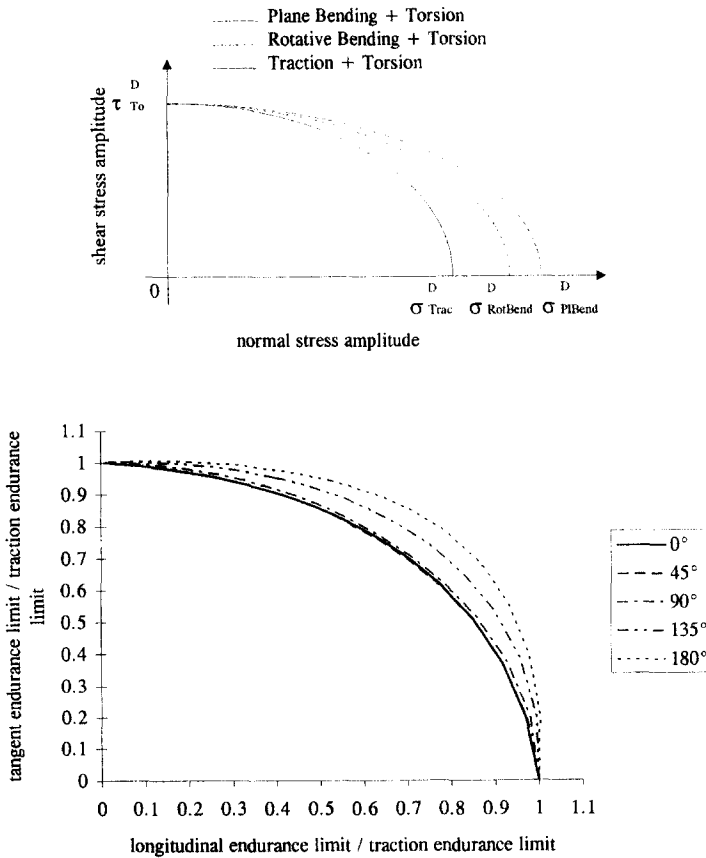$$\text{and} \quad \sigma_h^D = \frac{\sigma_l^D}{\lambda}$$

Fig. 5. – Predictions of the criterion in combined loadings and phase influence in biaxial traction.

6. Comparison between experiments and predictions

In order to test the accuracy of the predictions of our proposal, the comparison between experiments and predictions has been made for four materials and 14 experimental endurance limits on smooth cylindrical specimens. The materials are: a 30NCD16 quenched and tempered steel (Froustey and Lasserre, 1989), a XC18 annealed steel (Lasserre and Froustey, 1992), a 35CD4 quenched and tempered steel and a spheroidal graphite cast iron (AFNOR standard close to FGS800-2) (Bennebach, 1993) and (Palin-Luc, 1996). Their mechanical characteristics are given in Table I.

TABLE I. – Static mechanical characteristics of the tested materials.

Material	E (GPa)	υ	$Y_{0.02}$ (MPa)	$Y_{0.2}$ (MPa)	Sm (MPa)	Su (MPa)	A (%)
30NCD16 quenched & tempered	200	0.29	895	1080	1200	–	–
XC18 annealed	210	0.3	350	–	520	1530	24
35CD4 quenched & tempered	200	0.3	1015	1019	1123	–	13
FGS 800-2	164.9	0.275	320	462	795	815	9

E=Young modulus, υ=Poisson ratio, $Y_{0.02}$=Yield stress at 0.02%, $Y_{0.2}$=Yield stress at 0.2%, Sm=Maximum tensile stress, Su=Ultimate tensile stress, A=Elongation at failure.

For an objective and easy comparison the Relative Error of Prediction of the criterion, REP, is defined by (31).

$$(31) \qquad REP\,(\%) = \frac{\sigma^D_{\text{Experiment}} - \sigma^D_{\text{Prediction}}}{\sigma^D_{\text{Experiment}}} \times 100$$

All the REP are shown in Table II with the experimental data. The Table II proves that our criterion is in very good agreement with experiments. The absolute value of the REP is always less than 10%. Since crack propagation is not taken into account in the proposed criterion test results have to be relative to crack initiation detected as soon as possible with today experimental set up; for instance 0.5 mm in depth for a 12 mm diameter specimen with our multiaxial fatigue testing machine (Palin-Luc and Lasserre, 1994).

The values of σ^* given in Table II show that the ratio σ^*/σ^D_{Trac} varies between 0.7 and 0.9 for the five tested materials; we have not enough experimental data to generalize this observation.

7. Conclusion and prospects

This high cycle multiaxial fatigue criterion is the first to predict the experimental differences between traction, rotative bending and plane bending. These differences are

TABLE II. – Experimental results and relative error of prediction, REP, of the criterion.
The values in italics are used to identify the different parameters σ^* and β of the criterion.

Material	σ^*	β	Loading	σ^D (MPa)	τ^D (MPa)	σ^D/τ^D	φ (degree)	REP (%)
30NCD16	441	0.96	*Traction*	*560*	–	–	–	–
			Rotative bending	*658*	–	–	–	–
			Torsion	–	*428*	–	–	–
			Plane bending	690	–	–	–	–4.5
			Plane bending + torsion	519	291	1.78	0	–8.1
			Plane bending + torsion	514	288	1.78	90	–9.1
			Rotative bending + torsion	337	328	1.03	–	–8.3
			Rotative bending + torsion	482	234	2.06	–	–9.3
XC18	230	≈ 0	*Traction*	*273*	–	–	–	–
			Rotative bending	*310*	–	–	–	–
			Torsion	–	*186*	–	–	–
			Plane bending	332	–	–	–	–6.3
			Plane bending + torsion	246	138	1.783	0	1.6
			Plane bending + torsion	246	138	1.783	45	1.6
			Plane bending + torsion	264	148	1.783	90	8.3
35CD4	534	1.33	*Traction*	*558*	–	–	–	–
			Rotative bending	*581*	–	–	–	–
			Torsion	–	*384*	–	–	–
			Plane bending	620	–	–	–	4.3
FGS 800-2	204	3.09	*Traction*	*245*	–	–	–	–
			Rotative bending	*280*	–	–	–	–
			Torsion	–	*220*	–	–	–
			Plane bending	294	–	–	–	–9.2
			Plane bending + torsion	228	132	1.732	0	–7.2
			Plane bending + torsion	245	142	1.732	90	0.2
			Plane bending + torsion	199	147	1.35	0	–10.2

explained by the volumic distribution of the mean value on a cycle of the strain energy volumic density. Fully reversed loading modes are distinguished with this approach. The predictions of this criterion are in very good agreement with uniaxial and multiaxial experimental data on smooth cylindrical specimens in several materials. The criterion takes into account the difference between ductile and brittle materials by the β parameter. In the future the development of this method on notched specimens will be done by using the finite elements method to take into account the volumic distribution of the strain energy density around the notch. It is also necessary to take into account the influence of a mean value in a loading before this criterion can be adopted for design purposes. Nevertheless the capabilities of this method are very promising.

Acknowledgements

REFERENCES

BALLARD P., DANG VAN K., DEPERROIS A., PAPADOPOULOS Y. V., 1995, High cycle fatigue and finite element analysis, *Fatigue Fract. Engng. Mater. Struct.,* **18**, No. 3, 397-411.

BARRAULT J., LASSERRE S., 1980, Limites de fatigue de l'acier 35CD4 en flexion rotative et en flexion plane. *Rev. Mécanique Matériaux et Electricité,* Sept., 275-278.

BENNEBACH M., 1993, *Fatigue d'une fonte GS. Influence de l'entaille et d'un traitement de surface,* Ph. D. thesis, ENSAM CER de Bordeaux, France, 157 p.

DE LEIRIS H., 1969, Triaxialité des contraintes et critère de non fragilité, *Bulletin de l'Association Technique Maritime Aéronautique,* 481-491.

FROUSTEY C., LASSERRE S., 1989, Multiaxial fatigue endurance of 30NCD16 steel, *Int. J. Fatigue,* **11**, No. 3, 169-175.

FROUSTEY C., LASSERRE S., DUBAR L., 1992, Validité des critères de fatigue multiaxiale à l'endurance en flexion-torsion, *Mat-Tech 92,* 79-85, IITT-International, France.

GALTIER A., SÉGURET J., 1990, Critères multiaxiaux en fatigue : exploitation en bureau d'études. Proposition d'un nouveau critère, *Rev. Française Mécanique,* No. 1990-4, 291-299.

GOUGH H. J., POLLARD H. V., GLENSHAW W. J., 1951, Some experiments on the resistance of metals to fatigue under combined stresses, *Aeronaut. research council reports and memoranda,* 141 p., London.

LASSERRE S., FROUSTEY C., 1992, Multiaxial fatigue of steel-testing out of phase and in blocks: validity and applicability of some criteria. *Int. J. Fatigue,* **14**, No 2, 113-120.

LEMAITRE J., CHABOCHE J.-L., 1988, *Mécanique des matériaux solides.* Ed. Bordas, Paris, 544 p.

MASSONNET Ch., 1955, Le dimensionnnement des pièces de machines soumises à la fatigue. Contribution expérimentale à l'étude de l'effet de l'échelle et des entailles. *Rev. Univ. Mines,* Paris, **9**, T. XI, No. 6, 204-222.

MILLER K. J., ZACHARIAH K. P., 1977, Cumulative damage laws for fatigue crack initiation and stage I propagation, *J. Strain Analysis,* **12**, No. 4, 262-270.

PALIN-LUC T., LASSERRE S., 1994, Multiaxial fatigue testing machine under variable amplitude loading of bending and torsion. In *Recent Advances in Experimental Mechanics,* J. F. Silva Gomes *et al.* ed., Balkema A. A., Rotterdam, 965-970.

PALIN-LUC T., 1996, Fatigue multiaxiale d'une fonte GS sous sollicitations combinées d'amplitude variable. Ph. D. thesis, ENSAM CER de Bordeaux, France, 261 p.

PALIN-LUC T., LASSERRE S., BÉRARD J.-Y., 1997, Damage evolution of a spheroidal graphite cast iron loaded around its endurance limit. In *Proc. 5th Eur. Conf. on Advanced Materials and Processes and Applications,* SARTON L. A. J. L. and ZEEDJIK H. B. ed., Netherland Society for Material Science, Zwijndrecht, vol. 1, 511-514.

PAPADOPOULOS I. V., 1994, A new criterion of fatigue strength for out-of-phase bending and torsion of hard metals, *Int. J. Fatigue,* **16**, No. 6, 377-384.

PAPADOPOULOS I. V., PANOSKALTSIS V. P., 1994, Gradient dependent multiaxial high-cycle fatigue criterion, *Proc. 4th Int. Conf. Biaxial/Multiaxial Fatigue,* SF2M, St-Germain-en-Laye, France, Vol. 1, 461-476.

SIMBÜRGER A., 1975, Festigkeitsverhalten zäher Werkstoffe bei einer mehrachsigen, phasenverschobenen Schwingbeanspruchung mit körperfesten und veränderlichen Hauptspannungsrichtungen. Laboratorium für betriebsfestigkeit, Darmstadt, Germany, Bericht, Nr. FB-121, 89 p.

TSYBANEV G. V., 1994, An energy approach to fatigue tests and crack initiation stage determination. From *Problemy Prochnosti,* Ukranian Acad. Sci., Kiev. Plenum Publishing Corp., 2, 12-27.

VIVENSANG M., GANNIER A., 1994, Testing and microstructural interpretation of 35CD4 steels in cumulative high cycle fatigue damage. In *Recent Advances in Experimental Mechanics,* J. F. Silva Gomes *et al.* ed., Balkema A. A., Rotterdam, 1107-1112.